RETROGRADE SATELLITE FOR MONITORING GEOSYNCHRONOUS DEBRIS

Seiichiro KAWASE

Communications Research Laboratory
Kashima, Ibaraki 314-0012 Japan
E-mail: kawase@crl.go.jp

ABSTRACT *– An orbital geometry of a debris-monitoring satellite that enables orbit determination of target objects is described. A monitoring satellite with an on-board optical sensor is placed in a sub-synchronous, retrograde circular orbit. The satellite observes look-angles during encounters with the target objects that come into its field of view. Three encounters in 24 hours then determine the orbit of the target. Orbit determination accuracy is modeled as a function of the observation geometry parameters, including the look-angle resolution, observation field of view, and relative altitude of the orbits.*

KEYWORDS: Satellite-based optical tracking, Orbit determination error.

INTRODUCTION

In view of the particular importance of the spatial region of geosynchronous orbit (GSO) for telecommunication satellites, junk objects drifting in this region are a matter of concern. Ground-based optical sensors are currently able to detect GSO junk objects as small as one meter. However, detecting still smaller objects is recommended for better understanding the environment of GSO [1]. Meanwhile, a new detection technique is now being developed, that uses an optical sensor on board a monitoring satellite flying in a low altitude orbit [2]. If the monitoring-satellite orbit is high enough to be close to the GSO region, then smaller objects can be detected. Theoretical studies suggest that a close-up observation at a 1000-km range would enable detecting one-centimeter objects [3].

An orbital geometry that would appear reasonable for this close-up observation is illustrated in Fig. 1. The monitoring satellite revolves in a sub-synchronous, circular orbit. The satellite revolves at a faster rate than GSO target objects and observes targets one by one as it moves past them. Thus, the satellite completes one scan of the GSO region in one month, for example, if the relative altitude of the two orbits is 1000 km.

This "direct" orbital geometry has a drawback, however. Suppose that the monitoring satellite is passing a target, as illustrated in Fig. 2. Satellite M measures the look-angle u of a target T, in reference to the satellite's zenith Z. As M passes T, u will change from positive to negative. Now, suppose that there is another target T′ and its orbital altitude relative to M is twice that of T. The transversal motion of T′, relative to M, will then be twice the speed of T, while T′ will be twice the distance of T. So, if M passes T and T′ at the same time, the look-angles will show identically changing patterns for T and T′. Thus, the look-angles will not be able to distinguish T and T′. That is to say, the target's orbital radius is

16th International Symposium on Space Flight Dynamics, 3-7 December 2001, Pasadena, California, USA

indeterminable.

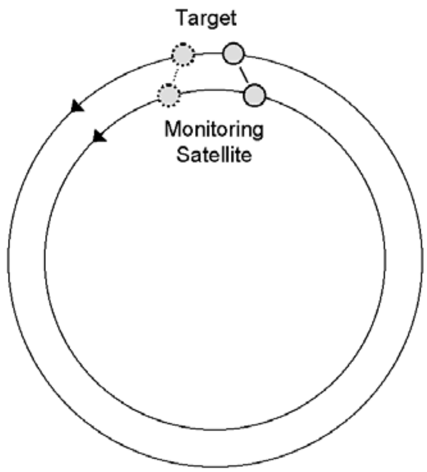

Fig. 1. Direct orbital geometry for monitoring.

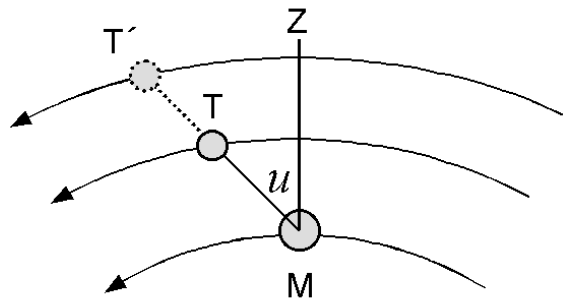

Fig. 2. Drawback of the direct geometry.

To solve this problem, this paper proposes a different orbital geometry, in which the revolution of the monitoring satellite is retrograde. We will show that this geometry enables the full determination of the target's six orbital elements. We will model the orbit determination error as a function of orbital geometry parameters and discuss the problems that arise particularly with our retrograde geometry.

ORBITAL GEOMETRY AND ENCOUNTER OBSERVATION

Assume that our monitoring satellite M is in a sub-synchronous, retrograde circular orbit and target object T is in a near-synchronous orbit. And assume, for the present, that M and T are in the equatorial plane. When M and T pass each other to make an encounter, as illustrated in Fig. 3, the u of T is measured at M, in reference to M's zenith Z. Because M and T fly in opposite directions, u changes fast. For example, if the relative orbital altitude h is 1000 km, the period of time that u remains within 45 degrees is 5.2 minutes. For comparison, suppose that we are at a ground station and observe a satellite that passes its zenith. If the satellite altitude is 1000 km, the period of time that the satellite remains within 45 degrees of the zenith is then 4.5 minutes, which is shorter than our retrograde encounter. If a ground-based optical observation works, then our encounter-based observation would also work.

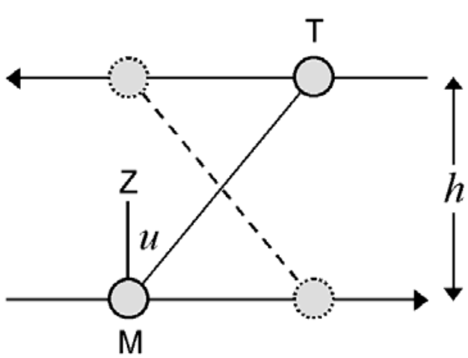

Fig. 3. Satellite-target encounter.

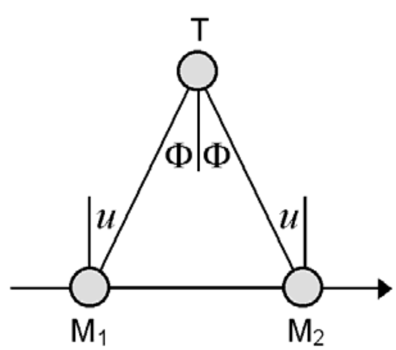

Fig. 4. Geometry of triangulation.

What is observed during one encounter is interpreted using Fig. 4. If we stood at T, then we would see as if M triangulates the position of T by measuring the look-angles at M_1 and M_2 as M passes T. Here, Φ denotes the field of view of the optical sensor. This Φ may include the stroke of the sensor's optical axis if it can be steered mechanically. Look-angle data will be taken at multiple points of time during one encounter, while the most significant data for the triangulation are those taken at the largest look-angle. So, we assume that we take look-angle data at M_1 and M_2.

The accuracy of the triangulation is analyzed in Fig. 5. Suppose that T is hypothetically displaced by δr towards the radial direction and by δl along the longitudinal direction. Correspondingly, the look-angle data u_1 and u_2, taken at M_1 and M_2, would deviate as:

$$\delta u_1 = (\delta r \sin\Phi + \delta l \cos\Phi) / (h / \cos\Phi)$$

$$\delta u_2 = (-\delta r \sin\Phi + \delta l \cos\Phi) / (h / \cos\Phi)$$

From these, we solve

$$\delta r = (\delta u_1 - \delta u_2)(h / \cos\Phi) / (2 \sin\Phi) \quad (1)$$

$$\delta l = (\delta u_1 + \delta u_2)(h / \cos\Phi) / (2 \cos\Phi) \quad (2)$$

Assume that δu_1 and δu_2 denote measurement noises and that the noises are non-correlated gaussian with standard deviation $\sigma\{u\}$. The standard deviations of δr and δl are then equal to

$$\sigma\{r\} = \varepsilon / (2^{1/2} \sin\Phi \cos\Phi) \quad (3)$$

$$\sigma\{l\} = \varepsilon / (2^{1/2} \cos^2\Phi) \quad (4)$$

Here, a quantity $\varepsilon = \sigma\{u\}h$ was introduced. This ε measures to what degree the look-angle resolves the target's transversal position (see Fig. 6). Note that δr and δl are non-correlated, as can be seen from equations (1) and (2).

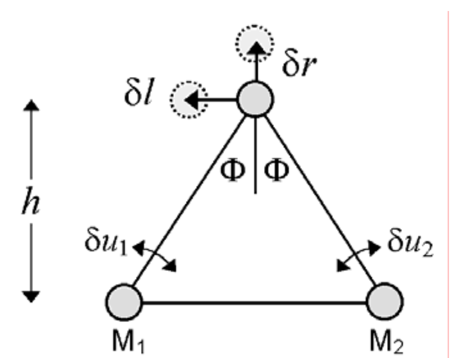

Fig. 5. Accuracy of triangulation.

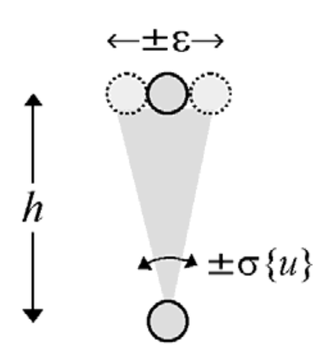

Fig. 6. Resolution power of the look-angle.

To summarize, the look-angle observation during one encounter yields one data set (r, l) with error-levels $\sigma\{r\}$ and $\sigma\{l\}$.

OBSERVATION EQUATIONS

We next consider how the observed (r, l) data are related to the target's orbit. The position of a near-synchronous target can be expressed relative to its reference stationary point. The reference point is 42,165 km away from the Earth's center, is directly above the equator, and is stationary with respect to the rotating earth. The target is assumed to be drifting near this reference point. Relative to the reference point, r measures the target's radial position and l the longitudinal position. The target's motion is then written in linearized terms, with a negligence of perturbations [4]:

$$r = -(2/3)D + E_1 \cos\theta + E_2 \sin\theta \quad (5)$$

$$l = L + D\theta - 2E_1 \sin\theta + 2E_2 \cos\theta \quad (6)$$

Here, the angle θ measures the earth's rotation. This angle goes beyond 2π because it also measures the lapse of time. An increase of 2π in θ corresponds to 23 hours 56 minutes, which is referred to as one day. The parameters L and D are for the target's longitudinal offset and drift-rate, and E_1 and E_2 are for a small orbital eccentricity. The set of L, D, E_1, and E_2 thus makes the orbital elements for discussing in-plane orbital motions.

Suppose that M has made a first encounter with T and acquired an observation data set (r_1, l_1). We can assume that the encounter has occurred instantaneously at $\theta = 0$. With this assumption, we write equations (5) and (6) in terms of variations to obtain the following observation equations.

$$\delta r_1 = -(2/3)\,\delta D + \delta E_1 \quad (7)$$

$$\delta l_1 = \delta L + 2\delta E_2 \quad (8)$$

Half a day later, M encounters T again. Correspondingly, from equations (5) and (6) with $\theta = \pi$, we have the following observation equations.

$$\delta r_2 = -(2/3)\,\delta D - \delta E_1 \quad (9)$$

$$\delta l_2 = \delta L + \pi\,\delta D - 2\delta E_2 \quad (10)$$

Precisely speaking, the second encounter occurs slightly earlier than $\theta = \pi$, because M revolves faster than T. But, this deviation could be regarded as being small here.

The third encounter occurs at $\theta = 2\pi$, for which similarly we have:

$$\delta r_3 = -(2/3)\,\delta D + \delta E_1 \quad (11)$$

$$\delta l_3 = \delta L + 2\pi\,\delta D + 2\delta E_2 \quad (12)$$

Observation equations (7-12) are understood as relating the errors in the observation data to the errors in the orbital elements.

ORBIT DETERMINATION ERRORS

We can now model the errors in orbit determinations. Suppose that we have acquired observation data from the first and second encounters. We then have four equations (7-10) and can determine:

$$\delta L = (\delta l_1 + \delta l_2) / 2 + 3\pi\,(\delta r_1 + \delta r_2) / 8$$

$$\delta D = -3(\delta r_1 + \delta r_2) / 4$$

$$\delta E_1 = (\delta r_1 - \delta r_2) / 2$$

$$\delta E_2 = (\delta l_1 - \delta l_2) / 4 - 3\pi\,(\delta r_1 + \delta r_2) / 16$$

These denote the orbit determination errors as being at the reference time $\theta = 0$. Calculating their standard deviations using equations (3) and (4) produces the error modeling:

$$\sigma\{L\} = 3\pi\varepsilon / (8 \sin\Phi \cos\Phi) \quad (13)$$

$$\sigma\{D\} = 3\varepsilon / (4 \sin\Phi \cos\Phi) \quad (14)$$

$$\sigma\{E_1\} = \varepsilon / (2 \sin\Phi \cos\Phi) \quad (15)$$

$$\sigma\{E_2\} = 3\pi\varepsilon / (16 \sin\Phi \cos\Phi) \quad (16)$$

In the calculations here, $1/\cos\Phi$ was neglected as being small compared with $1/\sin\Phi$. This is because the field of view Φ would tend to be small; otherwise the on-board observation hardware would be complex. The error modeling shows that smaller fields of view give rise to increased errors in every orbital element.

If our orbit determination uses three encounters, then we will have six equations (7-12) for determining δL, δD, δE_1, and δE_2. This is an "over-determined" case and so should be analyzed by using the least-squares method. However, the actual orbit determination will proceed as follows. Equations (3) and (4) show that the observed l is much more accurate than r. So, the data l_1, l_2, and l_3 will determine δL, δD, and δE_2 through equations (8), (10), and (12), regardless of r_1, r_2, and r_3. This results in

$$\delta L = (3\delta l_1 + 2\delta l_2 - \delta l_3) / 4$$

$$\delta D = (\delta l_3 - \delta l_1) / (2\pi)$$

$$\delta E_2 = (\delta l_1 - 2\delta l_2 + \delta l_3) / 8$$

Their standard deviations are calculated as

$$\sigma\{L\} = 7^{1/2}\, \varepsilon / (4 \cos^2\Phi) \tag{17}$$

$$\sigma\{D\} = \varepsilon / (2\pi \cos^2\Phi) \tag{18}$$

$$\sigma\{E_2\} = 3^{1/2}\, \varepsilon / (8 \cos^2\Phi) \tag{19}$$

After δL is known, any one of equations (7), (9), or (11) determines δE_1 as

$$\delta E_1 = \delta r_1 + (\delta l_3 - \delta l_1) / (3\pi)$$

Its standard deviation must be divided by $3^{1/2}$, because three equations over-determine δE_1. The result is

$$\sigma\{E_1\} = \varepsilon / (6^{1/2} \sin\Phi \cos\Phi) \tag{20}$$

Thus, the orbit determination errors were modeled for two-encounter and three-encounter cases, respectively, by equations (13-16) and equations (17-20). If the two cases are compared, the three-encounter case is much better because the factor $1/\sin\Phi$ is absent. Thus, putting the three-encounter orbital elements in a catalog of tracked objects is adequate. As is obvious from the discussions, orbit determination using one encounter is impossible.

OUT-OF-PLANE ORBITAL MOTION

Target objects may move away from the equatorial plane. If this motion is measured in z, it is written as

$$z = I_1\cos\theta + I_2\sin\theta \tag{21}$$

The elements I_1 and I_2 indicate an orbital inclination. This equation, together with (5) and (6) completes the linearized model of orbital motions. During an encounter, the target's z-position is observed through the look-angle v measured at the satellite in reference to the equatorial plane (see Fig. 7). In terms of variations, z and v are related by

$$h\, \delta v = \delta z \tag{22}$$

Consider the first encounter. Assuming $\theta = 0$ in equation (21) and using equation (22), we have

$$h\, \delta v_1 = \delta I_1 \tag{23}$$

We must time the second encounter correctly here. The orbital velocity (per unit θ) of the monitoring satellite is faster than the geosynchronous orbital velocity by $3h/2$. So, at $\theta = \pi$, the encounter is already over and the satellite is past the target by $3\pi h/2$. The encounter thus occurs at $\theta = \pi - \alpha$ (see Fig. 8), with $\alpha = 3\pi h/(4R)$ where R is the geosynchronous orbital radius. For example, α is 3.2 degrees if $h = 1000$ km.

The observation equation for $\theta = \pi - \alpha$, with a small α, thus becomes

$$h\delta v_2 = -\delta I_1 + \alpha\ \delta I_2 \tag{24}$$

Similarly, the third encounter occurs at $\theta = 2\pi - 2\alpha$, for which the observation equation becomes

$$h\delta v_3 = \delta I_1 - 2\alpha\ \delta I_2 \tag{25}$$

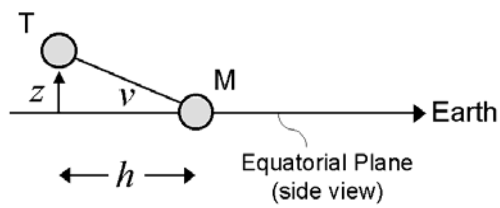

Fig. 7. Out-of-plane observation.

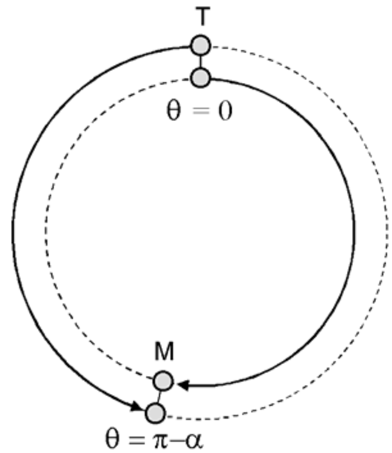

Fig. 8. Timing of the second encounter.

If our orbit determination uses two encounters, then equations (23) and (24) determine:

$$\delta I_1 = h\delta v_1$$

$$\delta I_2 = h\ (\delta v_1 + \delta v_2)\ /\ \alpha$$

Assuming that $\sigma\{v\} = \sigma\{u\}$, their standard deviations are

$$\sigma\{I_1\} = \varepsilon; \quad \sigma\{I_2\} = 2^{1/2}\ \varepsilon\ /\ \alpha$$

If two data points are acquired during each encounter, under our assumption, the total data points are twice that necessary for determining I_1 and I_2. So, the error modeling should be divided by $2^{1/2}$. Using α's value, we have

$$\sigma\{I_1\} = \varepsilon\ /\ 2^{1/2} \tag{26}$$

$$\sigma\{I_2\} = 4R\sigma\{v\}/(3\pi) \tag{27}$$

Thus, the I_2-error is much larger than the I_1-error.

If we use three encounters, then three equations (23-25) over-determine δI_1 and δI_2. But, note that the sensitivity for detecting δI_2 through equation (25) is twice that of equation (24). So, equations (23) and (25) practically determine the elements. Correspondingly, the error modeling becomes

$$\sigma\{I_1\} = \varepsilon\ /\ 2^{1/2} \tag{28}$$

$$\sigma\{I_2\} = 2R\sigma\{v\}/(3\pi) \tag{29}$$

Thus, the errors are modeled for all six orbital elements, using simple terms.

ORBITAL PREDICTION ERRORS

Orbital elements stored in the catalog will be used for predictions when re-acquiring a target becomes necessary. A re-acquisition will succeed if the position errors δl and δz are small enough when predicted. From equations (6) and (21), these position errors are written for a prediction interval θ:

$$\delta l = \theta\ \delta D - 2\delta E_1 \sin\theta$$

$$\delta z = \delta I_2 \sin\theta$$

Note here that the prediction will be over a long period; thus, the drift-error term becomes significant. To this, other significant error terms with δE_1 and δI_2 are added, thus making the above equations. Use $\sigma\{l\}$ to denote the standard deviation of δl. The upper bound of $\sigma\{l\}$ is then equal to $\theta\sigma\{D\} + 2\sigma\{E_1\}$. This upper bound is written, for the prediction interval of d days, as follows.

$$U_l(d) = \varepsilon\, d \,/\, (\cos^2\Phi) + 2\varepsilon \,/\, (6^{1/2} \sin\Phi \cos\Phi) \qquad (30)$$

Here, equations (18) and (20) are used. The predicted position may differ from the actual position as much as three times the standard deviation. Thus, a successful re-acquisition needs $3U_l(d) < h \tan\Phi$. This condition tells us until what date the catalogued elements can be used.

As for the error δz, its standard deviation changes periodically with θ, while its upper bound is:

$$U_z = \sigma\{I_2\} = 2R\sigma\{v\}/(3\pi) \qquad (31)$$

Equations (30) and (31) thus model the orbital prediction errors.

An example of the prediction error modeling is shown in Fig. 9. The assumed conditions are 1000 km for the relative altitude, 10 degrees for the field of view, and 0.1 degree for $\sigma\{u\}$ and $\sigma\{v\}$. The line marked with "D" is used for the first term of equation (30) as a reference. Meanwhile, orbital prediction errors are evaluated numerically, using the established covariance analysis and assuming the same conditions above. The numerical results are the undulating curves in the same figure. Our error modeling provides correct upper bounds to the numerical results.

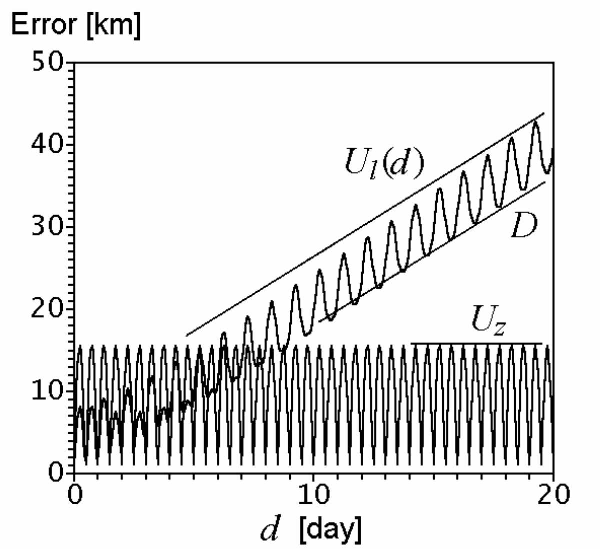

Fig. 9. Orbital prediction errors.

The two-encounter orbit determination was inaccurate for long-term predictions because of its unreduced drift-rate error. However, the determination will be usable for acquiring the target on the third encounter. Suppose we have determined a target's orbit from the first and second encounters. If we predict its position for the third encounter ($\theta = 2\pi$), it will have an error $\delta l = \delta L + 2\pi\ \delta D + 2\delta E_2$. The standard deviation of this error has the upper bound of $\sigma\{L\} + 2\pi\sigma\{D\} + 2\sigma\{E_2\}$. Therefore, the acquisition on the third encounter will succeed if the following condition holds.

$$3\,[\sigma\{L\} + 2\pi\sigma\{D\} + 2\sigma\{E_2\}] < h \tan\Phi$$

Substituting equations (13), (14), and (16) into this, we have

$$(27\pi / 4)\ \sigma\{u\} < \sin^2\Phi$$

Hence, a field of view greater than 6.2 degrees leads to a successful acquisition on the third encounter, if $\sigma\{u\} = 0.1$ degree and $h = 1000$ km.

PROBLEMS PARTICULAR TO RETROGRADE GEOMETRY

We have to identify, before starting observations on an encounter, which object in the field of view is our target if there are two or more. This is because the target object is unseen between encounters. This need for repeated identification is specific to our orbital geometry. Identification on the third encounter (and later encounters) will be supported by orbital predictions. Thus, the problem is how to identify our object on the second encounter.

To support this identification, we consider determining two orbital elements, I_1 and I_2, from the first encounter. Precisely speaking, the encounter begins at time $\theta = -\beta$, where $\beta = h \tan\Phi/(2R)$. This is illustrated in Fig. 10, where $(h / \cos\Phi)\ \delta v_1 = \delta z_1$ holds. So, from equation (21), we have one observation equation:

$$(h / \cos\Phi)\ \delta v_1 = \delta I_1 \cos\beta - \delta I_2 \sin\beta$$

Here, h is assumed nominally. β is small, so this equation can be written as

$$(h / \cos\Phi)\ \delta v_1 = \delta I_1 - \beta\ \delta I_2$$

Similarly, at the end of the encounter (time $\theta = \beta$), we have another equation:

$$(h / \cos\Phi)\ \delta v_2 = \delta I_1 + \beta\ \delta I_2$$

δI_1 and δI_2 are then determined and their standard deviations are calculated:

$$\sigma\{I_1\} = \varepsilon / (2^{1/2}\cos\Phi)\ ; \quad \sigma\{I_2\} = 2^{1/2} R\ \sigma\{v\}/ (\sin\Phi)$$

If the object's z-motion is predicted for the second encounter ($\theta = \pi - \alpha$), its error will be $\delta z = \alpha\ \delta I_2$ (note that the I_1-error is small), or $2^{1/2} 3\pi\ h\ \sigma\{v\}/(4 \sin\Phi)$ in standard deviation. Thus, the look-angle v can be predicted to within an error-level of $2^{1/2} 3\pi\sigma\{v\}/(4 \sin\Phi)$, which equals 1.9 degrees if $\sigma\{v\} = 0.1$ degree and $\Phi = 10$ degrees. We use this prediction for the identification.

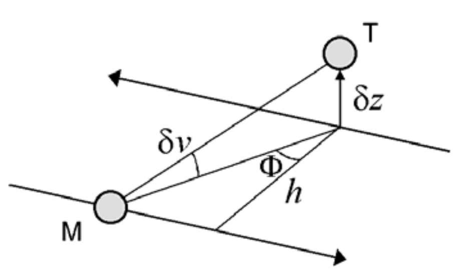

Fig. 10. Beginning of the first encounter.

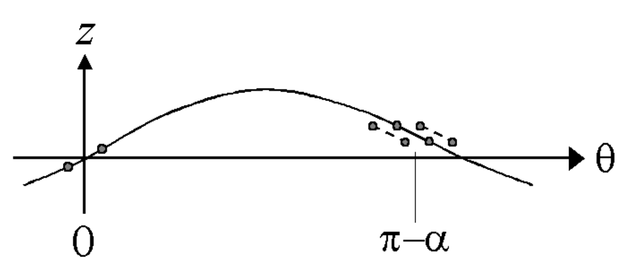

Fig. 11. Undulating z-position.

The identification will proceed as follows. The target's z-position will undulate with time due to an orbital inclination, as illustrated in Fig. 11. We determine the pattern of this undulation from the first encounter. We cannot determine the in-plane orbital elements, so we assume an ideally synchronous motion in the equatorial plane. We then vary its drift-rate, slightly increasing and decreasing h. Accordingly, the predicted pattern of z will be varied, as shown in Fig. 11 by the dotted lines. These z-predictions, including the variations, are then converted into look-angle predictions. An object that matches one of these predictions is then our object in question.

A target with a large orbital inclination introduces another problem. An encounter can then occur only when the target is crossing the equatorial plane. That is, two events must occur simultaneously: the target must cross the ascending or descending node, and the monitoring satellite must pass that node. These two events repeat in different periods, owing to the relative altitude h. Encounters will occur, but not frequently. Thus, observation chances are infrequent. This problem can be eased if the observational field of view is widened to the north and south. Using two or more sensors in a north-south array or one sensor with a north-south movable axis is thus recommended for the observation hardware. Selecting a larger h, which assures the safety-distance from GSO, also eases this problem.

In the planning of the monitoring mission, we will first determine the relative orbital altitude as large enough for safety. We will then determine the size and shape of the field of view, and design the orbit determination accuracy using our error models.

SUMMARY

It was shown that a sub-synchronous, retrograde monitoring satellite with an on-board optical sensor is able to determine the orbital elements of a target object from three-encounter observations. Errors in orbit determination and prediction were modeled in simple terms. Target identification procedures were suggested, and field-of-view requirements were pointed out.

REFERENCES

[1] National Research Council, "Orbital Debris; A Technical Assessment," National Academy Press, Washington DC, 1995.

[2] Sharma, J., "Space-Based Visible Space Surveillance Performance," Journal of Guidance, Control, and Dynamics, vol.23 (2000) pp.153-158.

[3] Takano, A., Kawaguchi, M., Arimoto, Y., Isobe, S., Tajima, T., Ichie, K., "A Preliminary Study on the On-Orbit Debris Observation System," 20th International Symposium on Space Technology and Science, 96-m-12, Gifu, Japan, May 19-25, 1996.

[4] Soop, E. M., Handbook of Geostationary Orbits, Kluwer, 1994.